Journal of Geography and Cartography 2024, 7(2), 9091.
https://doi.org/10.24294/jgc9091

Article

Assessing flood risk and vegetation dynamics: Implications for sustainable land management in Fars province

Amir Maleki[1], Alireza Naseri[2], Mohammadreza Yari[3], Faraz Estelaji[4], Rahim Zahedi[5,*], Seyyedeh Fatemeh Hosseini[6]

[1] Department of Civil, Water and Environmental Engineering, Shahid Beheshti University, Tehran, 1971733861, Iran
[2] Department of Transportation and Highway Engineering, Faculty of Civil and Environment Engineering, Amirkabir University of Technology, Tehran 1971733861, Iran
[3] Department of Construction Engineering, Faculty of Civil Engineering, Iran University of Science and Technology, Tehran 1971733861, Iran
[4] Department of Construction Engineering and Management, Faculty of Civil Engineering, Khajeh Nasir Toosi University, Tehran 1971733861, Iran
[5] Department of Renewable Energy and Environmental Engineering, University of Tehran, Tehran 1971733861, Iran
[6] Department of Geography and rural planning, Faculty of Urban Planning, Azad University, Science and Research Branch, Tehran 1971733861, Iran
*** Corresponding author:** Rahim Zahedi, rahimzahedi@ut.ac.ir

CITATION

Maleki A, Naseri A, Yari M, et al. Assessing flood risk and vegetation dynamics: Implications for sustainable land management in Fars province. Journal of Geography and Cartography. 2024; 7(2): 9091. https://doi.org/10.24294/jgc9091

ARTICLE INFO

Received: 12 September 2024
Accepted: 12 November 2024
Available online: 30 November 2024

Abstract: The design of effective flood risk mitigation strategies and their subsequent implementation is crucial for sustainable development in mountain areas. The assessment of the dynamic evolution of flood risk is the pillar of any subsequent planning process that is targeted at a reduction of the expected adverse consequences of the hazard impact. This study focuses on riverbed cities, aiming to analyze flood occurrences and their influencing factors. Through an extensive literature review, five key criteria commonly associated with flood events were identified: slope height, distance from rivers, topographic index, and runoff height. Utilizing the network analysis process within Super Decision software, these factors were weighted, and a final flood risk map was generated using the simple weighted sum method. 75% of the data was used for training, and 25% of it was used for testing. Additionally, vegetation changes were assessed using Landsat imagery from 2000 and 2022 and the normalized difference vegetation index (NDVI). The focus of this research is Qirokarzin city as a case study of riverbed cities, situated in Fars province, with Qir city serving as its central hub. Key rivers in Qirokarzin city include the Qara Aghaj River, traversing the plain from north to south; the primary Mubarak Abad River, originating from the east; and the Dutulghaz River, which enters the eastern part of the plain from the southwest of Qir, contributing to plain nourishment during flood events. The innovation of this paper is that along with the objective to produce a reliable delineation of hazard zones, a functional distinction between the loading and the response system (LS and RS, respectively) is made. Results indicate the topographic index as the most influential criterion, delineating Qirokarzin city into five flood risk zones: very low, low, moderate, high, and very high. Notably, a substantial portion of Qirokarzin city (1849.8 square kilometers, 8.54% of the area) falls within high- to very-high flood risk zones. Weighting analysis reveals that the topographic humidity index and runoff height are the most influential criteria, with weights of 0.27 and 0.229, respectively. Conversely, the height criterion carries the least weight at 0.122. Notably, 46.7% of the study area exhibits high flood intensity, potentially attributed to variations in elevation and runoff height. Flood potential findings show that the middle class covers 32.3%, indicating moderate flood risk due to changes in elevation and runoff height. The low-level risk is observed sporadically from the east to the west of the study area, comprising 12.4%. Analysis of vegetation changes revealed a significant decline in forest and pasture cover despite agricultural and horticultural development, exacerbating flood susceptibility.

Keywords: geographic information systems (GIS); flood risk analysis; network analysis process (NAP); weighted simple sum (WSS) method; sustainable development

1. Introduction

Flooding, inherently a natural phenomenon, often yields positive outcomes; however, its manifestation in urban environments entails devastating consequences, including property destruction and threats to human health. The escalation of population density, coupled with inadequate land use planning, deforestation, and the proliferation of impermeable surfaces, has impeded water infiltration in watersheds and accelerated downstream flow, exacerbating the frequency, intensity, and abruptness of urban floods, thereby affecting a growing number of individuals [1]. Spatial analysis offers a potent tool for examining dispersal patterns, enabling the establishment of logical relationships between human population distribution and environmental resources. Corrective measures for environmental risks and degraded lands hinge upon effective spatial planning [2]. Notably, recent years have witnessed extensive research endeavors both domestically and internationally, focusing on the assessment of flood risk sensitivity.

The analysis of floods in the United States, approached from a geomorphological standpoint and utilizing geographic information systems alongside a hierarchical analysis model, underscores the significant role played by geomorphological factors in flood occurrence within the region. Urban areas often employ impermeable surfaces as part of infrastructure development to augment runoff during heavy rainfall and flood events, consequently heightening flood susceptibility due to land use changes associated with urbanization [3]. A study spanning four years and employing a high-resolution monitoring network across eight catchments in southern England, encompassing both rural and urban locales, revealed discernible hydrological response disparities between the two settings. Notably, differences in runoff volume and flood response times were observed, with urbanization-induced alterations diverging from rural patterns [4]. Furthermore, soil moisture did not significantly impact runoff dynamics in urban areas, suggesting that spatial measurements of urbanization alone are sufficient predictors of flood occurrence in urban basins. The confluence of changes in rainfall patterns and land use further exacerbates urban areas' vulnerability to heavy rainfall and subsequent flooding [5]. In Egbaro state and Anambra state, topography and human alterations to riverbeds emerge as pivotal factors influencing flood risk. Flood risk assessment conducted in Bang Rakam, Thailand, utilizing a hierarchical analysis process (fuzzy) and incorporating eight flood risk assessment criteria (including distance from drainage networks, drainage density, water flow accumulation height, land slope, and average annual rainfall) revealed high flood risk concentrations near drainage networks with elevated ratings [6]. Notably, water flow accumulation height, water infiltration in soil, distance from drainage networks, medium drainage density, and basin land slope emerged as the most influential factors contributing to flood risk escalation in the region.

The vulnerability assessment of floods in Anambra, Nigeria, employing the network analysis process model, reveals a significant susceptibility of the state to flooding, with 73% of its total area classified as having medium to very high

vulnerability [7]. A study conducted in Bangladesh utilized Sentinel 1 and 2 satellite imagery to classify land use and assess flood-induced damage, revealing that approximately 23.98% of agricultural lands in Bangladesh have been adversely affected by recent floods. Zoning of flood risk potential within the Mardagh Chai catchment area, employing the network analysis process model, identifies slope and runoff height as the most critical factors, with weights of 0.3 and 0.28, respectively [8]. Conversely, lithology emerged as the least influential factor. Flood risk within this basin is contingent upon its physical characteristics [9]. In the West Islamabad catchment and its sub-basins, flood risk zoning utilizing the network analysis process model reveals that approximately 46% of the catchment area is deemed highly unsuitable. The West Islamabad catchment exhibits high flood capacity [10]. A flood vulnerability map for the Neka watershed of Sari city, utilizing a novel combined method of Bayesian theory and hierarchical analysis, identified areas of heightened flood sensitivity, particularly in the northern and northwestern regions characterized by dense human settlements and sparse vegetation cover. Flood zoning in Sari city, employing fuzzy analysis, indicates that the central and southern areas face the highest flood risk, with 12.24% of the mapped area falling into the very high-risk zone and 5.37% into the very low-risk zone [11]. Proposals to mitigate flood risk include retrofitting buildings along riverbanks to minimize flood damage. Qasimi et al. [12] aimed to assess landslide susceptibility in the Badakhshan province of Afghanistan, an area highly susceptible to landslides due to its complex topography and geological conditions. Koralay and Kara [13] chose the Söğütlü stream watershed in the Eastern Black Sea Region of Turkey as the study area to create a flood risk map using the Analytical Hierarchy Process and Weighted Overlay tools in ArcGIS.

In a separate study conducted in the Gomnabchai catchment area of Azerbaijan province, ten factors influencing flooding were identified using the network analysis process model. Results indicate that rainfall, land use, lithology, and slope are the most pivotal factors contributing to flood formation in the region [14]. Similarly, an investigation into the Qasimlu watershed in West Azarbaijan province, utilizing the network analysis process model, highlighted rainfall, distance from the river, and vegetation density as the primary influencing factors in flood occurrence. Notably, 22.82% of the study area was classified as having high to very high flood susceptibility [15]. Flood risk zoning of the Qatourchai watershed, employing a multi-criteria decision-making approach through the network analysis process and weighted linear combination model, revealed areas with a high potential for flooding, predominantly concentrated in the lower reaches of the basin. Waterways ranked 3 and 4 were identified as flood-prone zones, directing floodwaters downstream [16]. A spatial correlation analysis of vegetation cover changes and runoff height within the Gorganrood catchment area demonstrated that cities such as Agh Qola, Siminshahr, and Gomish Tepe, along with the Gorganrood River, are situated at high runoff elevations. Moreover, a significant negative spatial correlation (78%) between runoff height and vegetation density was observed, indicating a decline in forest and pasture cover from 1990 to 2021 [17]. Flood zoning of the Qarasu River in Golestan province, employing the analytic network process (ANP) method, identified topography, surface type, and vegetation as the principal factors influencing flooding in the region [18].

As a result of the literature, an increase in the likelihood and adverse impacts of flood events is expected. Therefore, concentrated action is needed at the regional level to avoid severe impacts on human life and property. In order to have an effective tool available for information on flood risk, as well as a valuable basis for priority setting and further technical, financial, and political decisions regarding flood risk mitigation and management, it is necessary to establish flood risk maps that show the potential adverse consequences associated with different flood scenarios.

Riverbed cities have a historical record of recurrent floods, spanning various periods. These inundations resulted in human casualties, agricultural land damage, disruption of transportation routes, and destruction of urban infrastructure, including buildings and gardens. The flood of 2018 in Qirokarzin city, for instance, incurred significant financial losses amounting to $4,826,151. Given this context, the present research endeavors to identify the primary criteria governing flood occurrences in Qirokarzin city, with a particular focus on exploring the relationship between floodplain distribution and changes in vegetation cover. The main innovation of this paper is that, along with the objective to produce a reliable delineation of hazard zones, a functional distinction between the loading and the response system (LS and RS, respectively) is made.

2. Methodology

2.1. Case study

The focus of this research is Qirokarzin city as a case study of riverbed cities, situated in Fars province, with Qir city serving as its central hub. Geographically, Qirokarzin city spans from longitude 52 degrees 6 minutes to longitude 53 degrees 13 minutes east and latitude 28 degrees 32 minutes to latitude 28 degrees 54 minutes north (**Figure 1**) [19]. The city covers an area of 339,547 hectares, with an elevation of 750 meters above sea level. Over eleven years, the average annual rainfall in the region amounts to 319.6 mm, with the highest rainfall occurring in February (86.6 mm) and the lowest in June (0 mm). The average highest and lowest temperatures are recorded in July (34.1 degrees Celsius) and January (12.4 degrees Celsius), respectively. According to Dumarten's classification, the study area falls within a dry climate zone [20]. Elevations range from a maximum of 2187 meters in the north to a minimum of 314 meters in the south and central regions of the city. Notably, key rivers in Qirokarzin city include the Qara Aghaj River, traversing the plain from north to south; the primary Mubarak Abad River, originating from the east; and the Dutulghaz River, which enters the eastern part of the plain from the southwest of Qir, contributing to plain nourishment during flood events. The construction of the Bitumen Reservoir Dam in the northeast of Qir city, situated on the Qara-Aghaj River, is a notable feature of the area's hydrological infrastructure [21]. From a soil science perspective, the predominant soil type across much of the study area is classified as antisol. Land use analysis reveals that approximately 15,370 hectares are designated as second-grade pastures, while third-grade pastures cover about 216,553 hectares [22]. Agricultural lands occupy an estimated area of 44,861 hectares. Additionally, approximately 59,505 hectares of Qirokarzin city's area are forested, with the remaining land use comprising rocky terrain devoid of vegetation, as well as areas designated for urban

and village boundaries, transportation routes, water bodies, and miscellaneous uses. **Figure 2** shows a photo of the flood in the area.

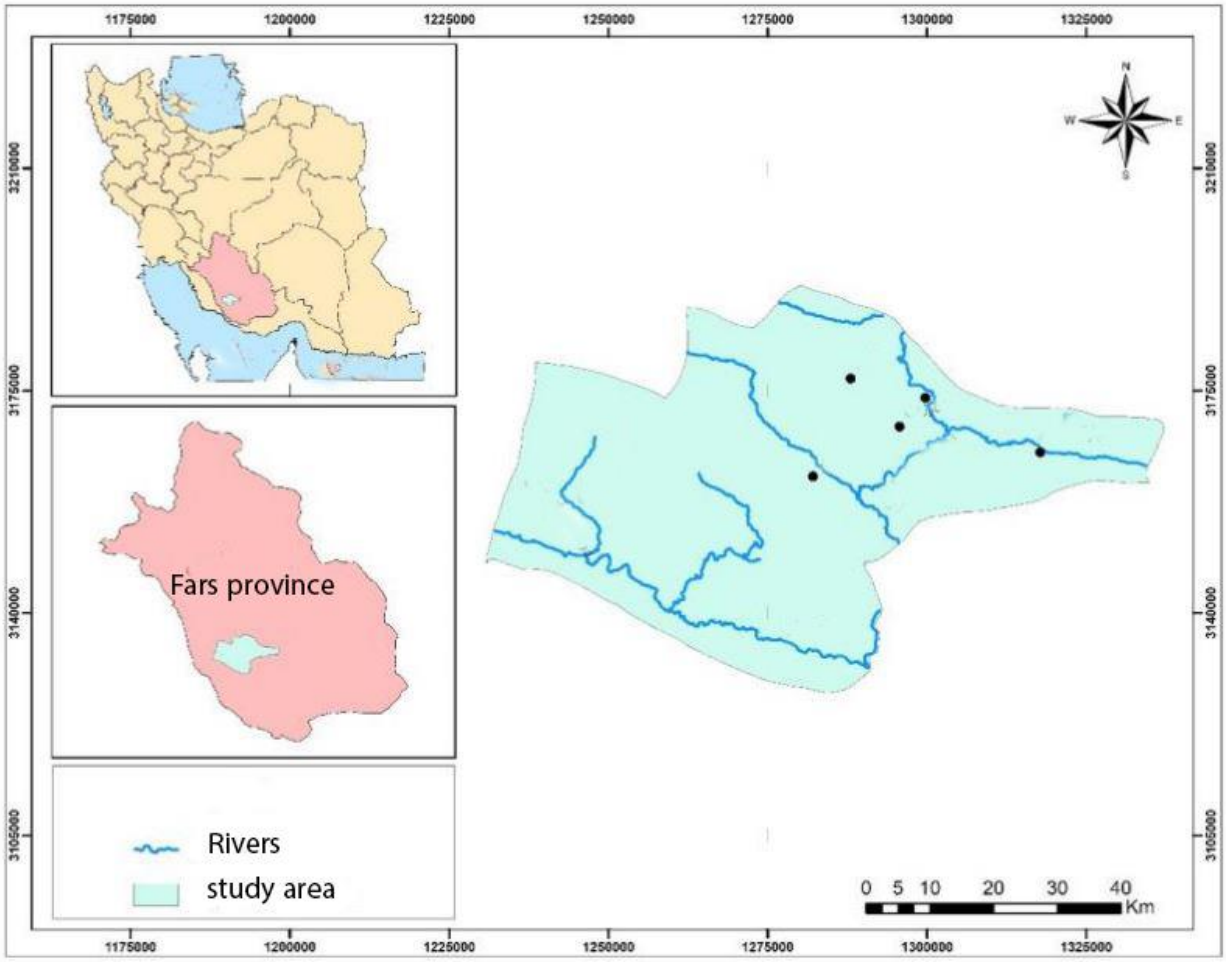

Figure 1. Location of Qirokarzin city in Fars province.

Figure 2. Qirokarzin city's flood photo.

2.2. Vegetation difference index

The analysis of vegetation changes reveals notable shifts in the normalized vegetation difference index values between 2000 and 2021 across the study area (**Figures 3** and **4**). The increase in these index values indicates a proliferation of vegetation, primarily driven by agricultural and horticultural expansion, particularly along the Hengam and Qara-Aghaj rivers, as well as in the vicinity of Mubarak Abad, Imam Shahr, and Qir cities. However, this expansion of agricultural activities has come at the expense of natural vegetation, leading to the conversion of low-density forests into pastures and the degradation of once robust pastures into weaker ones with minimal coverage. Consequently, the diminishing forest and pasture vegetation have resulted in reduced water infiltration and increased runoff, exacerbating the risk of flooding in the area. Furthermore, the expansion of agricultural lands along riverbanks has left them susceptible to flooding during periods of heavy rainfall. Moreover, the absence of vegetation on agricultural lands for certain parts of the year renders them more susceptible to erosion compared to forest and pasture lands. This heightened erosion leads to soil fertility depletion and loss of vegetation cover.

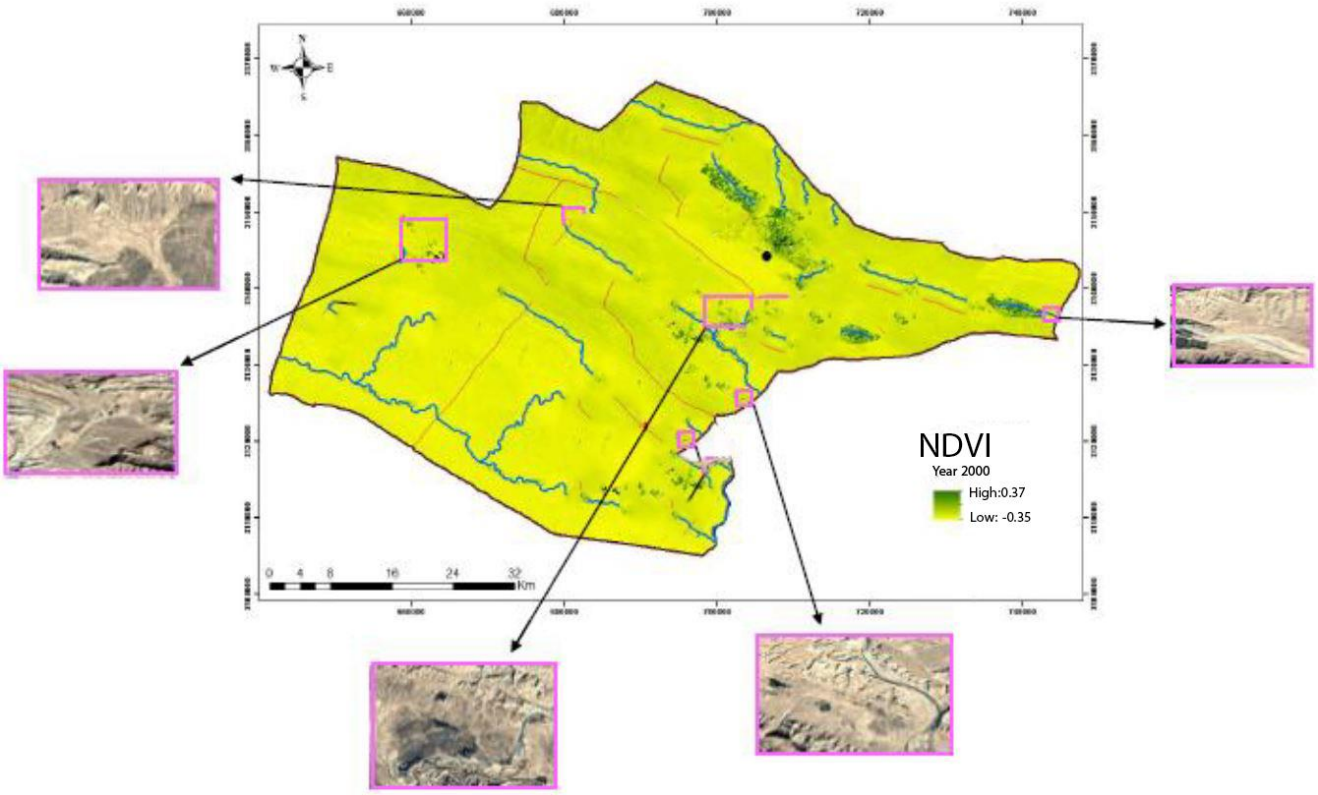

Figure 3. The normalized vegetation difference index in the year 2000.

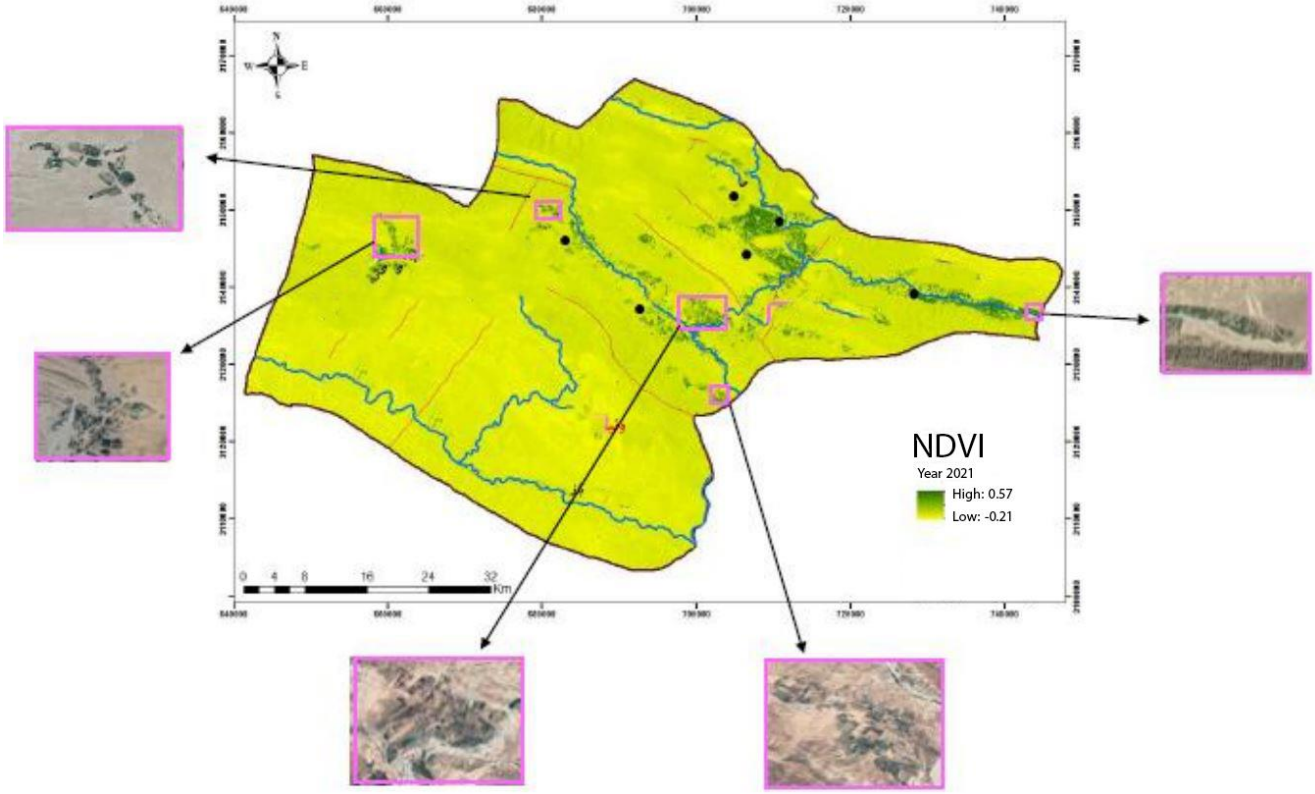

Figure 4. The normalized vegetation difference index in the year 2021.

To facilitate flood zoning in Qirokarzin city, the following approach was undertaken: Initially, a comprehensive review of literature alongside field visits was conducted to identify key factors influencing flood occurrences in the study area. Subsequently, a multi-criteria decision model was employed, integrating both primary and secondary data sources. The primary dataset included a digital elevation model (DEM) with a resolution of 101 meters, derived from topographic data with a scale of 1: 25,000. Additionally, slope data, obtained from the DEM, and a fundamental geological map with a scale of 1:100,000 were incorporated into the analysis. Furthermore, average rainfall data spanning a 30-year period and a map delineating soil hydrological groups were utilized to enhance flood zoning accuracy. In order to assess vegetation status and estimate changes over a 21-year timeframe, Landsat 8 and Landsat 7 satellite images from the years 2000 and 2021 were employed. The normalized difference vegetation index (NDVI) was utilized to analyze vegetation dynamics within Qirokarzin city, providing valuable insights into vegetation trends and alterations over the specified period.

The normalized difference vegetation index (NDVI) is a widely utilized indicator in vegetation change monitoring. It is calculated using Equation (1) [23].

$$\mathrm{NDVI} = \frac{\mathrm{NIR} - \mathrm{RED}}{\mathrm{NIR} + \mathrm{RED}} \tag{1}$$

In this context, NIR represents the spectral reflectance of the near-infrared band, while RED signifies the spectral reflectance of the red band. The normalized difference vegetation index (NDVI) ranges from −1 to +1. For green vegetation, the normalized plant difference index typically falls within the range of approximately 0.1

to 0.8, indicating greenness and high plant density. Thus, this index serves as an effective indicator for assessing plant growth and distribution. Following the preparation of Landsat imagery for the study area, vegetation quantity and density were extracted within the ArcGIS software environment.

2.3. Network analysis process model

The network analysis process model stands out as a prominent and practical decision-making tool, emphasizing the interdependence among criteria. Initially proposed by Chemweno et al. [24] in 2015, this model provides a structured framework for decision-making and problem evaluation. It delineates a network of connections between elements across different clusters, encompassing both external dependencies and internal connections within a cluster. Essentially, the network analysis process model elucidates the interrelationships among components, facilitating a comprehensive understanding of complex systems. One of the key advantages of the network analysis process model is its applicability to both qualitative and quantitative scenarios, offering a versatile approach to addressing various issues and challenges [25]. By employing this model, it becomes feasible to overcome interconnected issues and optimize decision-making processes. Given the significance of flood control and mitigation, understanding the factors influencing floods is paramount for effective planning and management. Prior knowledge of these factors enables proactive measures to be implemented, enhancing flood control efforts and minimizing potential damages. The process of executing the network analysis process model typically involves the following steps:

The process of executing the network analysis process model typically involves the following steps [26]:

(1) Building the analysis model:

- Identify criteria influencing the final decision and establish connections between them to form a network structure.
- Develop pairwise comparison matrices to evaluate the impact of criteria and sub-criteria, considering higher levels of the network and internal communication.
- Calculate the weight vector W using Equation (2), where λ_{max} represents the largest eigenvalue of matrix A. The compatibility index (CI) of the criteria weight is utilized to determine the degree of compatibility of comparisons, as calculated by Equation (3). If CI is less than 0.1, the comparisons are deemed acceptable.

$$AW = \lambda_{max} W \tag{2}$$

$$CI = \frac{\lambda_{max} - n}{n - 1} \tag{3}$$

(2) Forming the primary supermatrix.

(3) Forming the weighted supermatrix:

- Utilize the Super Decision software to calculate the dependencies and generate the weighted supermatrix.

(4) Calculation of the general weighted vector of the limit of the supermatrix:

- Ensure convergence of the weighted supermatrix to its limit power, where the elements of the convergent matrix and its row values are equal.

In this study, maps and information layers for each element were prepared using ArcGIS software. Subsequently, the final coefficients obtained from the network analysis process were applied to each layer. Finally, the simple weight sum method was employed to generate the final map.

The topographic index represents the degree of flow accumulation at any point within a catchment area, indicating the tendency of water to move downhill under the influence of gravity. In Equation (4), A is the specific catchment area, measured in square meters per meter, and β is the slope of the pixel, measured in degrees.

$$TWI = \ln\left(\frac{A_s}{\tan\beta}\right) \tag{4}$$

Topography serves as a crucial factor influencing the spatial distribution of saturated areas and driving changes in hydrological conditions within a watershed. It significantly impacts soil moisture distribution, with underground water flow often closely following surface topography [27]. The topographic moisture index is a valuable tool for assessing moisture conditions at the watershed scale, influenced by flow direction and cumulative flow [28]. Flow direction dictates the transfer of water from one cell to another, while flow accumulation describes the concentration of runoff from various elevation points, guided by the slope and shape of the terrain [29]. Consequently, areas with abundant waterways in the catchment area exhibit high levels of accumulation. The topographic moisture index assigns numerical values to landscapes, with lower values indicating dry cells and higher values signifying wet cells [30]. Threshold values are determined through classification methods, incorporating local knowledge of basin characteristics and observations of local responses to heavy precipitation and surface runoff. These criteria are applied to the output raster, facilitating comprehensive analysis of water flow dynamics on the Earth's surface.

The American Soil Conservation Organization's rainfall-runoff model, established subsequent to Sherman's 1949 studies on rainfall-runoff relationships, is a commonly utilized method in hydrology. This model aims to generate a single hydrograph representing the correlation between rainfall and runoff [31]. To determine the volume of rainfall converted into runoff, it is imperative to ascertain the rainfall depth within the study area. Runoff volume is directly proportional to flood magnitude; as runoff depth increases, the likelihood of flooding escalates, whereas a reduction in runoff depth corresponds to a decreased flood risk. Equation (5) is employed to compute the maximum potential for rainfall retention in centimeters [32].

$$S = \frac{2500}{\mathrm{CN} - 254} \tag{5}$$

The calculation of Curve Number (CN) involves factors such as soil hydrological groups, land productivity, hydrological conditions of the land, and previous soil moisture status of the region. CN values range from zero to 100, with zero indicating no runoff production [33]. As the CN value increases, the runoff volume also increases. At a CN value of 100, all rainfall is converted into runoff [34]. Ultimately, the height of runoff in the study area can be determined based on layers representing

the maximum rainfall retention potential of the land and the thirty-year average rainfall of Qirokarzin, using Equation (6).

$$Q = \frac{(P - 0.2S)^2}{P + 0.8S} \tag{6}$$

Q is the runoff height in millimeters.

P is the average annual precipitation in millimeters.

S is the maximum potential of land precipitation retention.

The proposed procedural map is shown in **Figure 5**. The first step (sub-procedure A) in the proposed procedural roadmap consists of determining consistent flood hazard and risk scenarios. The specific aims are to obtain a spatially explicit representation of the frequency and magnitude (intensity) for each of the underlying hazard scenarios and to quantify the associated consequences in terms of losses with respect to values exposed, and thus risk. The main result is the so-called risk reference prospect, which serves as a basis for a performance comparison between possible risk mitigation alternatives. In this paper, emphasis is put on the computational aspects needed to derive flood risk.

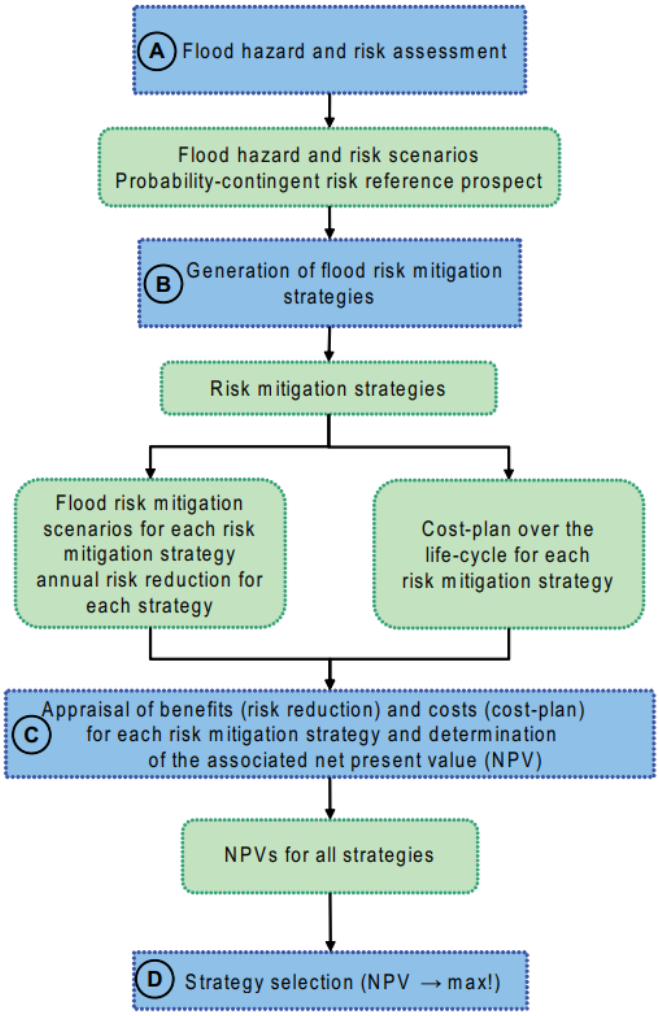

Figure 5. Procedural roadmap for a comprehensive risk mitigation project assessment.

3. Results and discussion

In analyzing the spatial distribution of flooding and vegetation changes in Qirokarzin city, maps depicting criteria such as slope height, distance from the river, topographic moisture index, and runoff height were generated. The results of the benchmark map are presented below:

3.1. Slope height

Altitude significantly influences various environmental factors such as rainfall patterns, evaporation rates, temperature, hydrology, runoff, soil conditions, and vegetation. There exists an inverse relationship between altitude and flooding, with higher elevations associated with reduced flood risk. The slope height criterion map illustrates that as elevation increases, the likelihood of flooding decreases, whereas flooding probability rises with decreasing elevation. Qir, Imam Shahr, Mubarak Abad, and Afzer are situated at lower altitudes, posing a higher risk of flooding. Notably, major rivers in the study area, including the Baz River, Hengama, Tang Kish, and Qara Aghaj, flow through these low-lying areas, contributing to their elevated flood risk.

Overall, the analysis of slope height provides valuable insights into flood vulnerability across Qirokarzin city, highlighting areas at heightened risk due to their lower elevations and proximity to major water bodies. **Figure 6** illustrates the standard slope map within the city, aiding in visualizing the terrain characteristics and their impact on flood susceptibility.

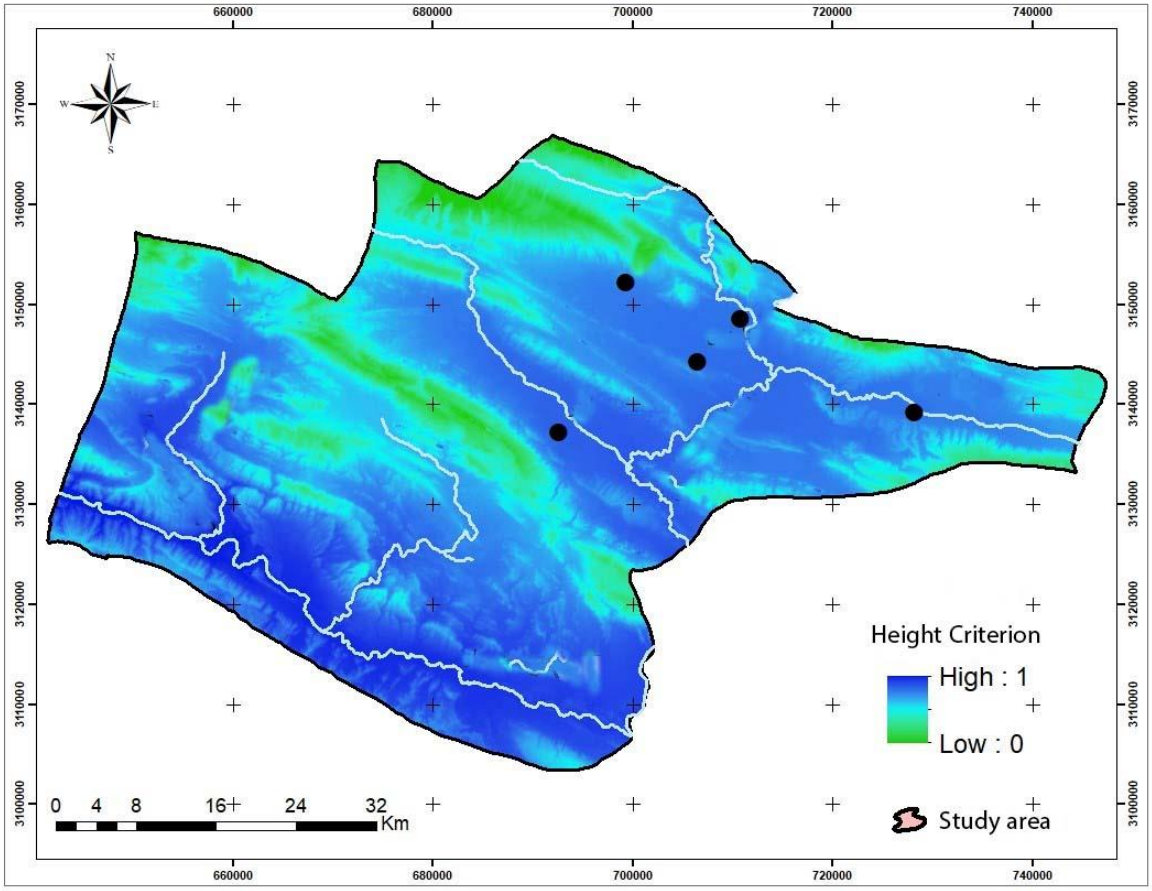

Figure 6. The standard slope height map.

3.2. Slope

The slope criterion exhibits an inverse relationship with the likelihood of flooding. Areas with higher slopes tend to experience decreased flood probabilities, whereas those with lower slopes are at higher risk of flooding. A standard map of slope within the study area was prepared to visualize this relationship (**Figure 7**). Analysis indicates that cities such as Qir, Imam Shahr, Mubarak Abad, and Afzer are situated in regions with low slopes, indicating a higher flood risk. Notably, major rivers, including Baz, Hengama, Tang Kish, and Qara-Aghaj, are located in areas with the lowest slope, correlating with the highest probability of flooding.

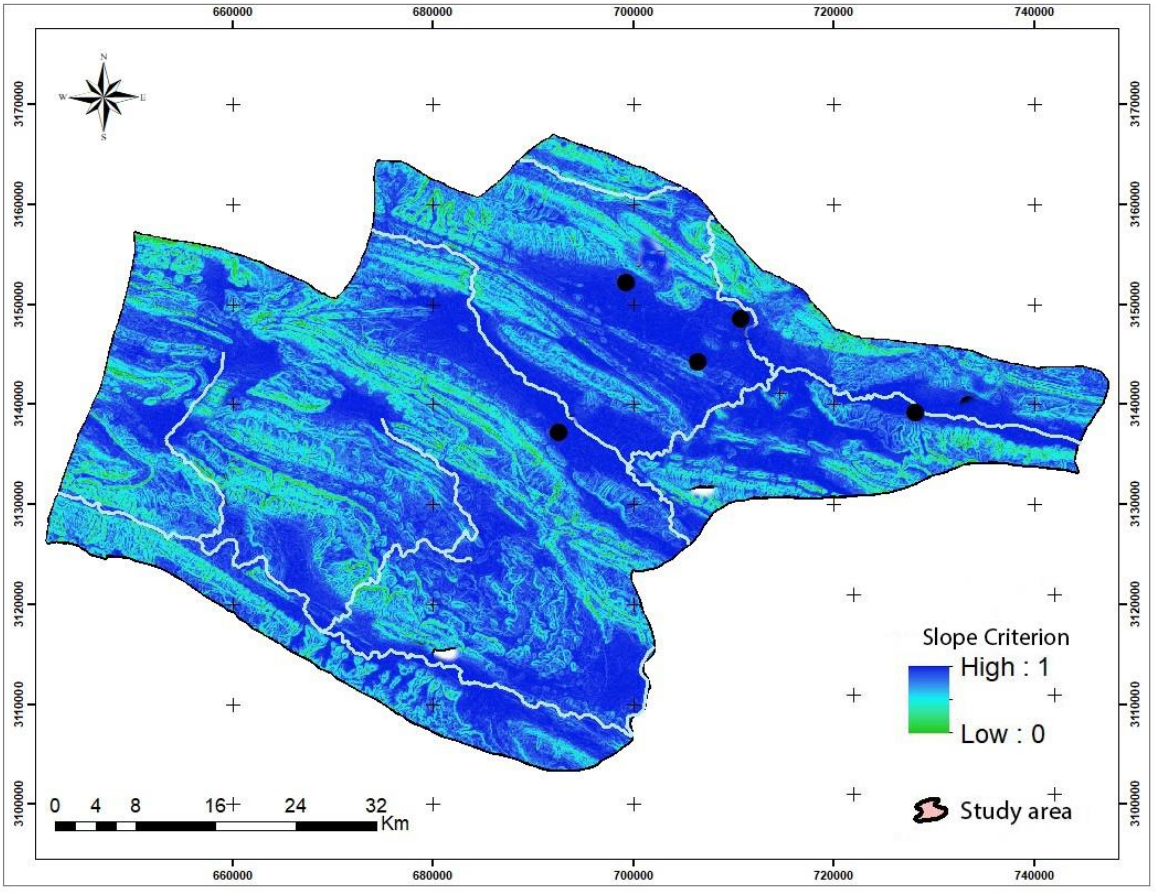

Figure 7. Standard map of slope criterion.

3.3. Distance from river

Flooding occurs when rainwater exceeds the soil and vegetation's absorption capacity, and the natural river channel cannot accommodate the runoff. Higher values on the distance from the river map signify a greater flood probability closer to the riverbed, while flood probability decreases with distance from the riverbed. Hence, the distance from the river criterion directly influences flood probability. Analysis reveals that cities like Qir, Imamshahr, Mubarakabad, and Afzer are at risk of flooding due to their proximity to the main riverbed (**Figure 8**). Additionally, the main rivers Baz, Hengama, Tang Kish, and Qara-Aghaj exhibit the highest probability of flooding within their beds.

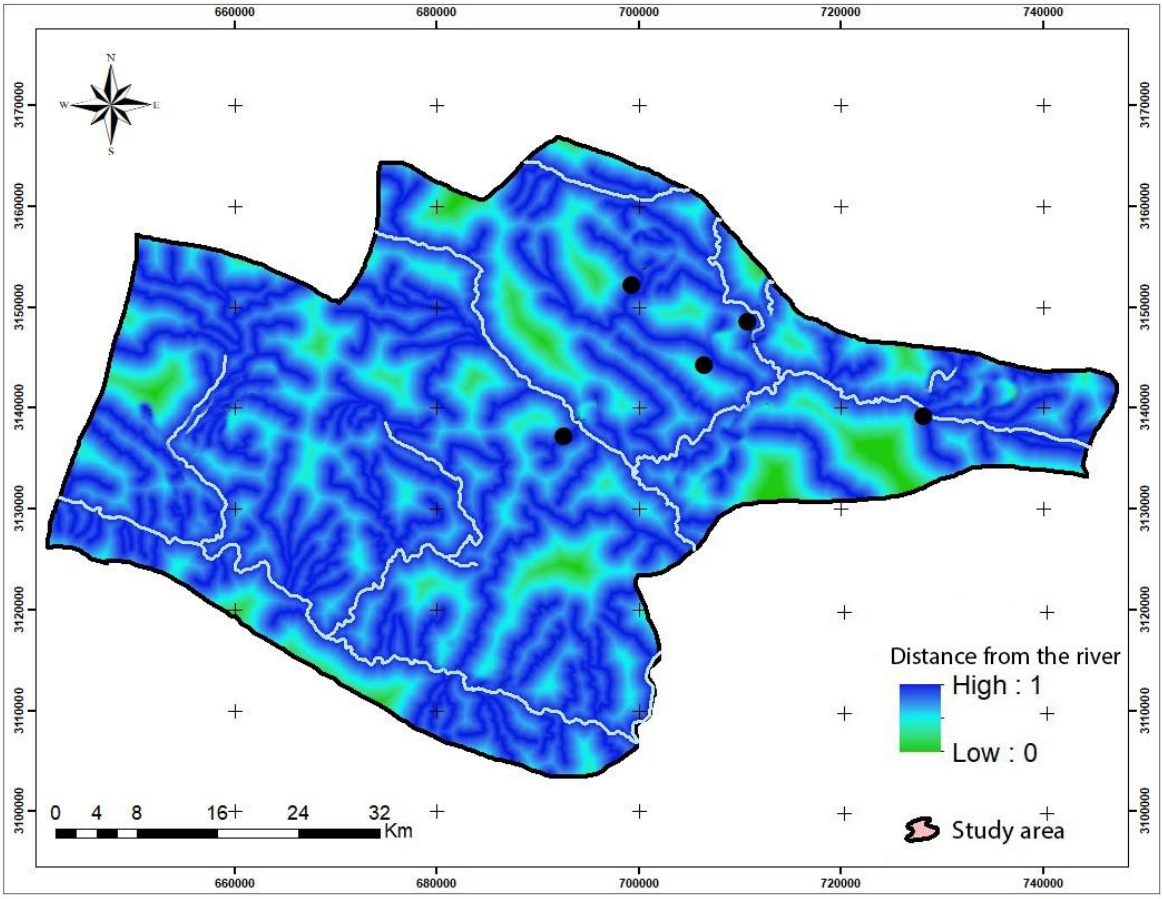

Figure 8. map of distance from the river criterion.

3.4. Topographic moisture index

The topographic moisture index is directly related to floods. Analysis of the topographic moisture index within the study area reveals significant insights into flood susceptibility. In valleys and depressions, where the index reaches its highest value of one, there is increased flow accumulation and soil moisture. Conversely, in ridge areas characterized by low flow accumulation and dry soil conditions, the index attains its lowest value of zero (**Figure 9**). This spatial distribution of the topographic moisture index provides valuable information about areas prone to flooding, with higher values indicating elevated flood risk due to increased flow and soil moisture. Conversely, lower values indicate reduced flood risk associated with drier soil conditions and limited flow accumulation.

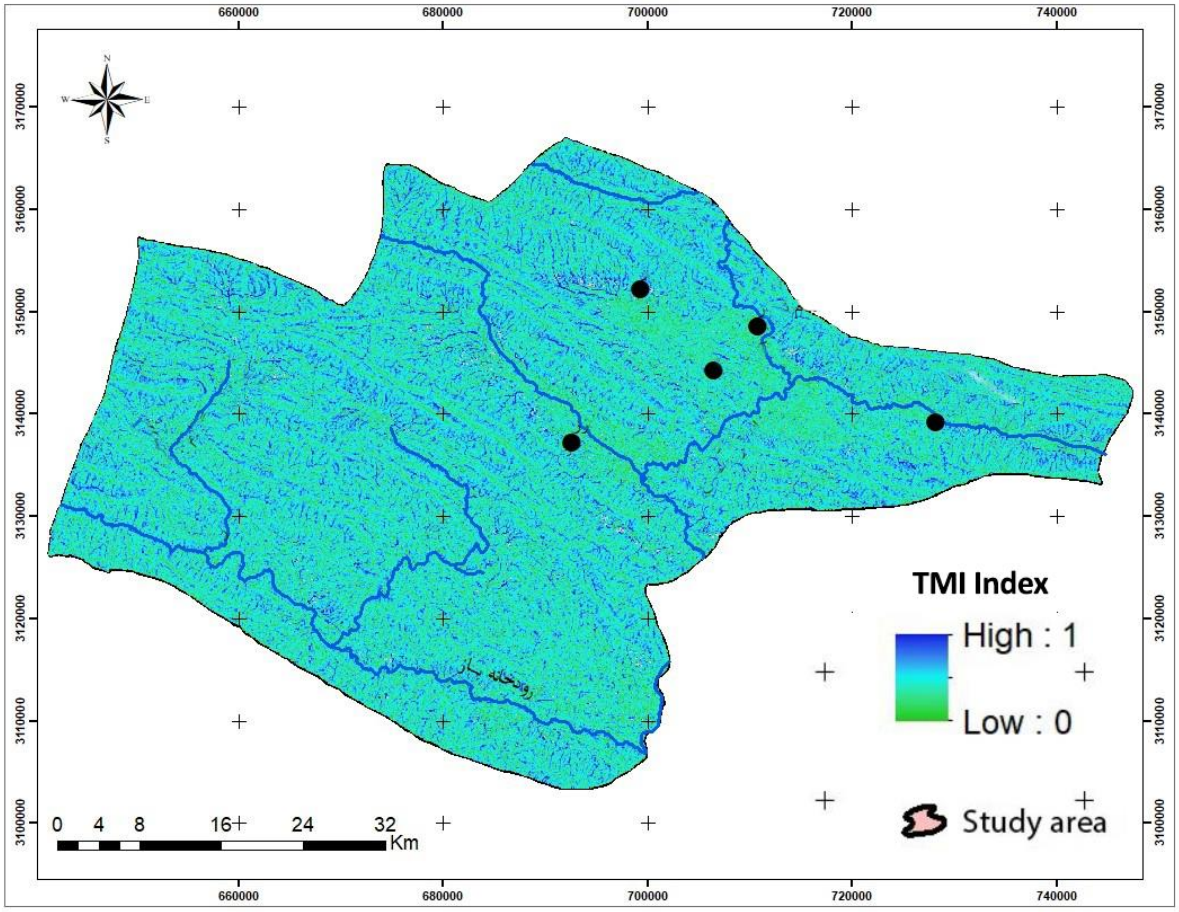

Figure 9. Topographic Moisture Index map.

3.5. Runoff height

The analysis of runoff height provides crucial insights into flood vulnerability within the study area. Observations reveal that the maximum runoff height is concentrated at the headwaters of rivers, denoted by a value of 1 with Imam Shahr located in this region (**Figure 10**). In these areas, soil infiltration is high, leading to minimal runoff production. Conversely, green areas indicate locations where all rainfall is absorbed into the soil, resulting in no runoff. Furthermore, within the riverbeds of major rivers such as Roodkhane Baz, Hengam, and Qara Aghaj, the runoff height reaches its highest calculated value, indicating the highest probability of flooding in these areas. As distance from the main rivers increases, the probability of flooding decreases. Notably, the Tang Kish River exhibits lower runoff height compared to other major rivers, suggesting a relatively lower flood risk in its vicinity.

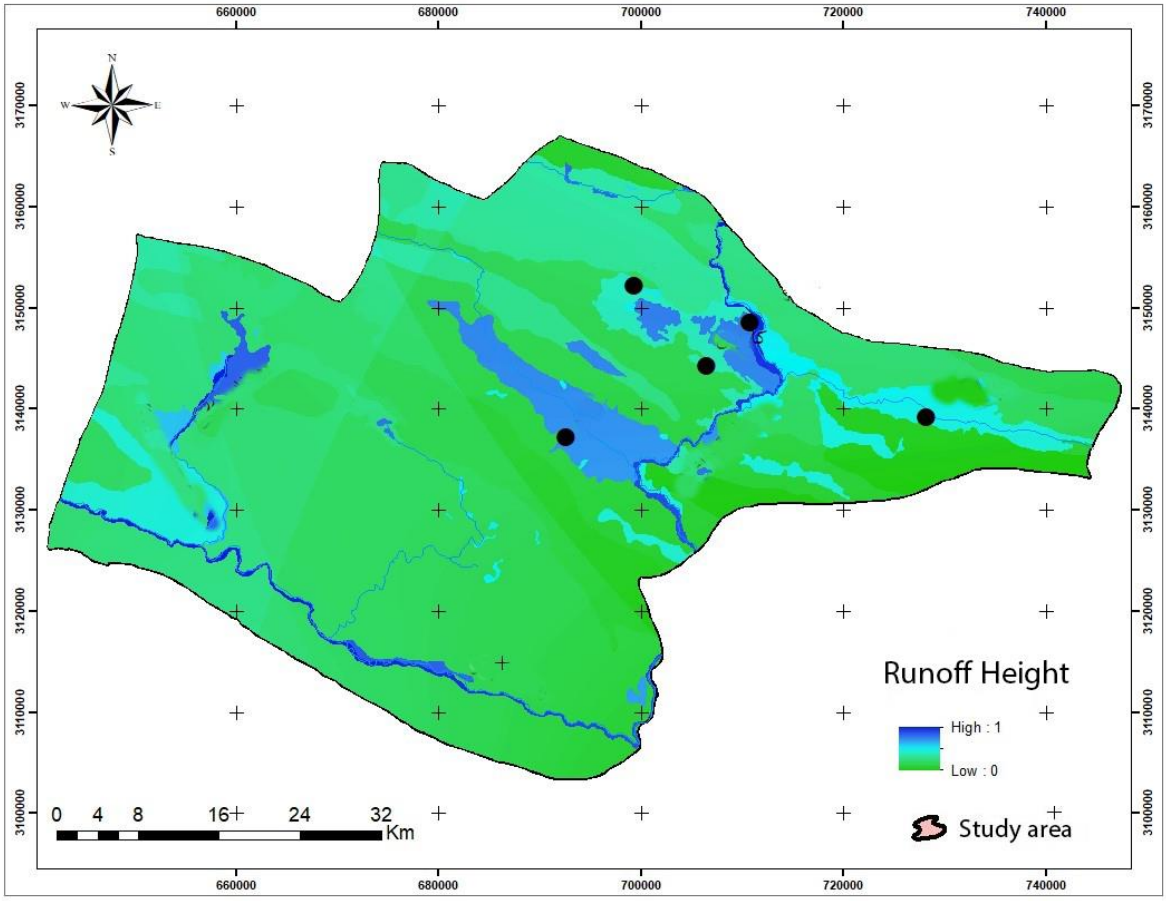

Figure 10. Runoff height map.

3.6. Weighting criteria

The analysis reveals the weighting of criteria within Qirokarzin city, with the topographic moisture index criterion holding the highest weight of 0.27 and the height criterion having the lowest weight of 0.122. Additionally, the distance from the Shib River and the height of the runoff in the study area hold weights of 0.183, 0.196, and 0.229, respectively. The weight of each criterion affecting the flood occurrence is shown in **Table 1**.

Table 1. Weight of each criterion affecting the flood occurrence.

	Criteria	Weight
1	Slope Height	0.122
2	Slope	0.196
3	Distance from the River	0.183
4	Topographic Moisture Index	0.270
5	Runoff Height	0.229

3.7. Flood potential analysis

The risk of flooding within the study area is categorized into five levels: very low, low, medium, high, and very high (**Figure 11**). **Table 2** provides details on the area and percentage of each flood occurrence class. Notably, five primary areas, along

with several sub-areas, exhibit a very high flood risk. These areas are predominantly situated in the central, southern, northeastern, and northwestern regions of the study area. Cities such as Imam Shahr and Afzer face a high risk of flooding, particularly along major rivers like Baz, Hengam, Qara Aghaj, and parts of the Tang Kish riverbed. The distribution of strata with a high probability of flooding is scattered throughout the study area. Qir, Karzin, and Mubarak Abad are located within high flood risk zones, with a significant portion of the Tang Kish riverbed also facing high flood risk. This class encompasses the largest area, covering 157,730.1 hectares (46.7 percent) of the study area. Furthermore, the middle class covers an area of 108,946.1 hectares (32.3 percent), indicating moderate flood risk due to changes in elevation and runoff height. The low-level risk is observed sporadically from the east to the west of the study area, comprising 41,746.7 hectares (12.4 percent). Finally, very low-risk areas are minimal and primarily located in the eastern and northern regions of the study area, where increased elevation and slope contribute to reduced flood probability.

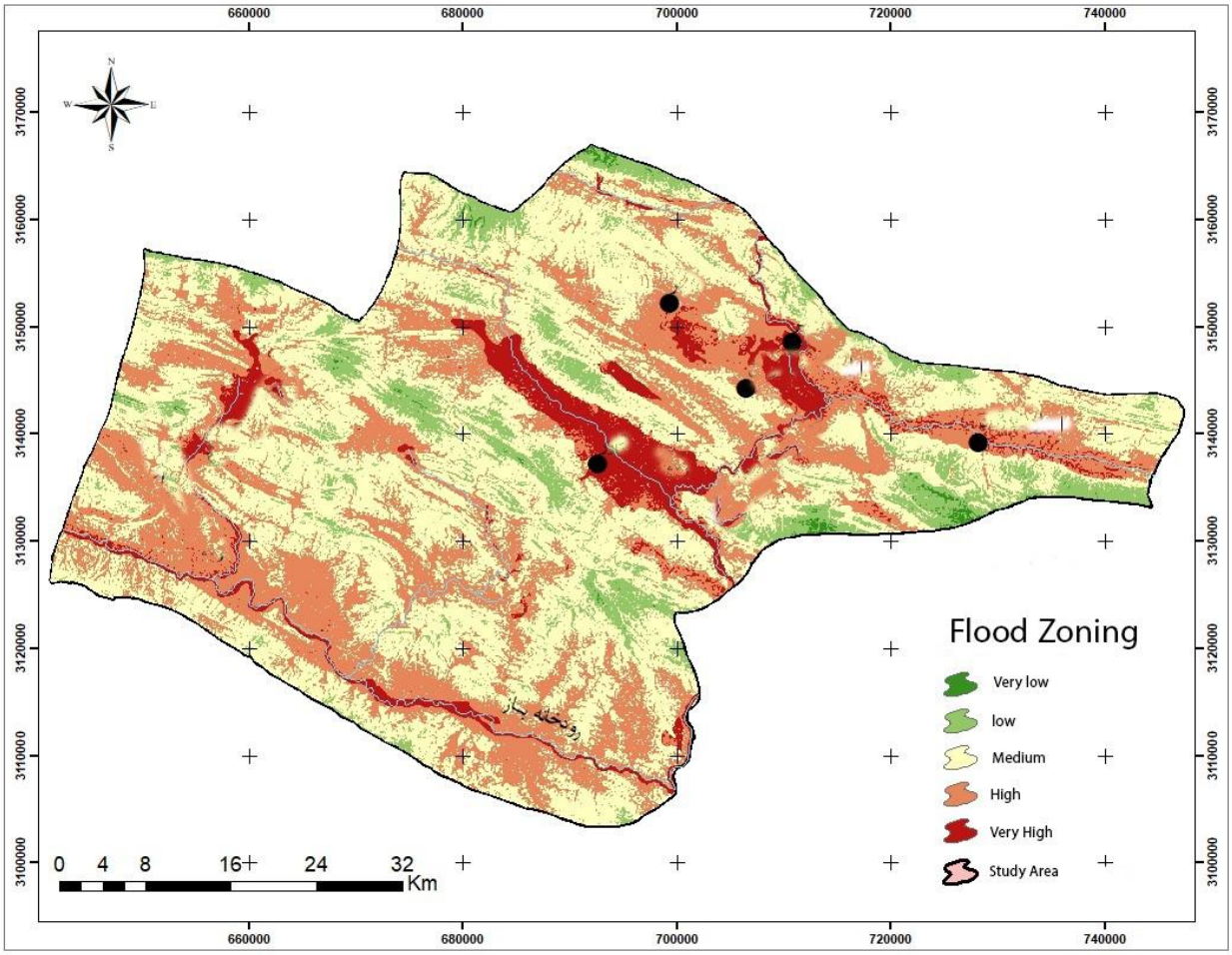

Figure 11. Flood zoning map.

The spatial distribution results reveal that areas with high and very high flood risk are dispersed across three sections of the study area characterized by low altitude and slope. During heavy rainfall events, the adjacent elevations to these areas play a critical role in generating runoff and peak discharge. Additionally, the geological composition of the study area, dating back to the late third and fourth geological

periods, contributes to a very low infiltration rate, often leading to hazardous floods. Moreover, the presence of gravel and stones in floodwaters enhances their force, resulting in greater erosion of riverbeds and channel banks and even causing significant damage to houses located nearby.

Table 2. Area and percentage of flood risk.

Flood Risk	Area (hectares)	Percentage
Very Low	1933.6	0.5
Low	41,746.7	12.4
Medium	108,946.1	32.3
High	157,730.1	46.7
Very High	27,230.7	8.1

3.8. Vegetation changes analysis

In areas lacking vegetation, heavy rainfall events result in significant water flow down mountain slopes, often culminating in hazardous floods. The presence of soil erosion, sediment-laden water, and debris such as sand, rubble, and stones increases the force of floodwaters, causing severe erosion of riverbeds and channel banks and even the destruction of nearby houses. Overall, the analysis underscores the intricate relationship between vegetation dynamics, land use changes, soil erosion, and flood risk, highlighting the urgent need for sustainable land management practices to mitigate the adverse impacts of flooding in the study area.

The findings of this study echo those of previous research on the spatial correlation between vegetation changes and runoff height, as evidenced in the Gorgan River catchment. A study on this catchment revealed a 78% spatial correlation between vegetation and runoff height, indicating a negative relationship between these variables [35]. Similarly, in our study area, human-induced land use changes, such as deforestation, pasture degradation, and agricultural expansion, have contributed to reduced vegetation cover and increased runoff height. Comparing the distribution of flooding and vegetation changes over the study period highlights the prevalence of agricultural areas in high flood-risk zones. Emphasizing the importance of vegetation density and sustainable land use practices, previous research on the Shiraz dry river basin underscores the role of preserving natural land cover in mitigating floods. Alterations in land use upstream have been shown to decrease flood delay times by 50%, elevating flood risks. Moreover, our research aligns with studies utilizing hierarchical analysis models to assess flood risk. For instance, a study employing lithological precipitation, drainage density, land slope, and land use criteria identified high and very high flood-risk zones, predominantly situated in upstream areas. Similarly, satellite imagery analysis of Qirokarzin revealed dense vegetation in agricultural lands, consistent with our vegetation change findings.

4. Conclusion

Floods pose a significant threat in the world, including Iran, where historical records and observations underscore the recurring nature of this hazard. Vegetation dynamics play a pivotal role in influencing flood patterns, influenced by a myriad of

factors. This study investigates flood risk in Qirokarzin city in relation to vegetation changes, identifying five critical criteria: height, slope, distance from the river, topographic humidity, and runoff height. Weighting analysis reveals that the topographic humidity index and runoff height are the most influential criteria, with weights of 0.27 and 0.229, respectively. Conversely, the height criterion carries the least weight at 0.122. Notably, 46.7% of the study area exhibits high flood intensity, potentially attributed to variations in elevation and runoff height. The presence of the bitumen reservoir dam in a flood-prone area raises concerns regarding overflow risks during peak periods, warranting further research into flood risk management strategies.

Analysis of vegetation changes from 2000 to 2022 indicates a significant expansion of agriculture. Despite the rise in the normalized difference vegetation index (NDVI), flood intensity remains unabated. Spatial analysis reveals a weak correlation (Pearson coefficient: 0.320) between flood intensity and NDVI changes, emphasizing the primacy of upstream land management practices over vegetation improvements in flood mitigation efforts. The findings underscore the imperative of proactive watershed management, focusing on soil conservation, runoff infiltration, and flood control in upstream areas. Redirecting management efforts towards protection, soil conservation, and enhanced runoff infiltration can yield more sustainable flood mitigation outcomes. Further research into flood risk dynamics and vegetation changes is warranted to inform evidence-based flood management strategies in Qirokarzin city and similar regions.

Investigations into rural-urban settlements indicate over 70% vulnerability to floods in developed areas, emphasizing the need for management measures. These include vegetation preservation in upstream areas, maintaining safe distances from riverbeds during urbanization, watershed management to extend flood concentration times, and public awareness initiatives to promote nature-friendly practices and sustainable land use patterns. By integrating these findings into flood risk management strategies, there’s potential to reduce vulnerability and enhance resilience to flooding in Qirokarzin city and similar regions. Analysis of the alike areas morphology, channel confinement, and the analysis of present land use maps, as well as exploratory investigation to anticipate future land demands and land use change, can be conducted in future studies.

Author contributions: Conceptualization, AM and RZ; methodology, AN; software, MY; validation, FE, SFH and AM; formal analysis, RZ; investigation, AM; resources, AN; data curation, MY; writing—original draft preparation, FE; writing—review and editing, SFH; visualization, AM; supervision, RZ; project administration, AN; funding acquisition, MY. All authors have read and agreed to the published version of the manuscript.

Conflict of interest: The authors declare no conflict of interest.

References

1. Few R, Matthies F. Flood hazards and health: responding to present and future risks. Taylor & Francis; 2013.

2. Melo-Merino SM, Reyes-Bonilla H, Lira-Noriega A. Ecological niche models and species distribution models in marine environments: A literature review and spatial analysis of evidence. Ecological Modelling. 2020; 415: 108837. doi: 10.1016/j.ecolmodel.2019.108837
3. Guria R, Mishra M, Dutta S, et al. Remote sensing, GIS, and analytic hierarchy process-based delineation and sustainable management of potential groundwater zones: a case study of Jhargram district, West Bengal, India. Environmental Monitoring and Assessment. 2023; 196(1). doi: 10.1007/s10661-023-12205-6
4. Sauquet E, Shanafield M, Hammond JC, et al. Classification and trends in intermittent river flow regimes in Australia, northwestern Europe and USA: A global perspective. Journal of Hydrology. 2021; 597: 126170. doi: 10.1016/j.jhydrol.2021.126170
5. Oudin L, Salavati B, Furusho-Percot C, et al. Hydrological impacts of urbanization at the catchment scale. Journal of Hydrology. 2018; 559: 774–786. doi: 10.1016/j.jhydrol.2018.02.064
6. Yousefi H, Moradi S, Zahedi R, et al. Developed analytic hierarchy process and multi criteria decision support system for wind farm site selection using GIS: A regional-scale application with environmental responsibility. Energy Conversion and Management: X. 2024; 22: 100594. doi: 10.1016/j.ecmx.2024.100594
7. Chukwuma EC, Okonkwo CC, Ojediran JO, et al. A GIS based flood vulnerability modelling of Anambra State using an integrated IVFRN-DEMATEL-ANP model. Heliyon. 2021; 7(9): e08048. doi: 10.1016/j.heliyon.2021.e08048
8. Zahedi R, Sadeghitabar E, Khazaee M, et al. Potentiometry of wind, solar and geothermal energy resources and their future perspectives in Iran. Environment, Development and Sustainability. 2024. doi: 10.1007/s10668-024-04633-2
9. Ghanbarpour MR, Saravi MM, Salimi S. Floodplain Inundation Analysis Combined with Contingent Valuation: Implications for Sustainable Flood Risk Management. Water Resources Management. 2014; 28(9): 2491–2505. doi: 10.1007/s11269-014-0622-2
10. Johnston R, Smakhtin V. Hydrological Modeling of Large river Basins: How Much is Enough? Water Resources Management. 2014; 28(10): 2695–2730. doi: 10.1007/s11269-014-0637-8
11. Tien Bui D, Khosravi K, Shahabi H, et al. Flood Spatial Modeling in Northern Iran Using Remote Sensing and GIS: A Comparison between Evidential Belief Functions and Its Ensemble with a Multivariate Logistic Regression Model. Remote Sensing. 2019; 11(13): 1589. doi: 10.3390/rs11131589
12. Qasimi AB, Isazade V, Enayat E, et al. Landslide susceptibility mapping in Badakhshan province, Afghanistan: a comparative study of machine learning algorithms. Geocarto International. 2023; 38(1). doi: 10.1080/10106049.2023.2248082
13. Koralay N, Kara Ö. Assessment of flood risk in Söğütlü stream watershed of Trabzon province in Turkey using geographic information systems and analytic hierarchy process approach. Natural Hazards. 2024; 120(11): 9977–10000. doi: 10.1007/s11069-024-06594-1
14. Estelaji F, Moniri N, Yari MH, et al. Earthquake, flood and resilience management through spatial planning, decision and information system. Future Technology. 2024; 3(2): 11–21. doi: 10.55670/fpll.futech.3.2.2
15. Khah MV, Zahedi R, Mousavi MS, et al. Forecasting renewable energy utilization by Iran's water and wastewater industries. Utilities Policy. 2023; 82: 101546. doi: 10.1016/j.jup.2023.101546
16. Mehrzad K, Rahim Z, Reza F, et al. Potential assessment of renewable energy resources and their power plant capacities in Iran. Global Journal of Ecology. 2022; 7(2): 060–071. doi: 10.17352/gje.000062
17. Goodarzi MR, Niknam ARR, Sabaghzadeh M. Rainfall-runoff modeling using GIS: A case study of Gorganrood Watershed, Iran. Water Resource Modeling and Computational Technologies. 2022; 165–181. doi: 10.1016/b978-0-323-91910-4.00011-x
18. Taherizadeh M, Niknam A, Nguyen-Huy T, et al. Flash flood-risk areas zoning using integration of decision-making trial and evaluation laboratory, GIS-based analytic network process and satellite-derived information. Natural Hazards. 2023; 118(3): 2309–2335. doi: 10.1007/s11069-023-06089-5
19. Estelaji F, Aghajari AA, Zahedi R. Flood zoning and developing strategies to increase resilience against floods with a crisis management approach. Asian Review of Environmental and Earth Sciences. 2023; 10(1): 14–27. doi: 10.20448/arees.v10i1.4439
20. Estelaji F, Naseri A, Keshavarzzadeh M, et al. Potential measurement and spatial priorities determination for gas station construction using WLC and GIS. Future Technology. 2023; 2(4): 24–32. doi: 10.55670/fpll.futech.2.4.3

21. Estelaji F, Naseri A, Zahedi R. Evaluation of the Performance of Vital Services in Urban Crisis Management. Advances in Environmental and Engineering Research. 2022; 03(04): 1–19. doi: 10.21926/aeer.2204057
22. Mirzavand H, Aslani A, Zahedi R. Environmental impact and damage assessment of the natural gas pipeline: Case study of Iran. Process Safety and Environmental Protection. 2022; 164: 794–806. doi: 10.1016/j.psep.2022.06.042
23. Pettorelli N. The normalized difference vegetation index. Oxford University Press; 2013.
24. Chemweno P, Pintelon L, Van Horenbeek A, et al. Development of a risk assessment selection methodology for asset maintenance decision making: An analytic network process (ANP) approach. International Journal of Production Economics. 2015; 170: 663–676. doi: 10.1016/j.ijpe.2015.03.017
25. Dwyer L, Gill A, Seetaram N, et al. Handbook of research methods in tourism: Quantitative and qualitative approaches. Edward Elgar Publishing; 2012.
26. Teng J, Jakeman AJ, Vaze J, et al. Flood inundation modelling: A review of methods, recent advances and uncertainty analysis. Environmental Modelling & Software. 2017; 90: 201–216. doi: 10.1016/j.envsoft.2017.01.006
27. Liu S, Wang Y, An Z, et al. Watershed spatial heterogeneity of soil saturated hydraulic conductivity as affected by landscape unit in the critical zone. CATENA. 2021; 203: 105322. doi: 10.1016/j.catena.2021.105322
28. Ghorbani M, Ghaderi N, Estelaji F, et al. Evaluating Surface Water Collection Infrastructure for Management of Urban Flood Risk: Integrating HEC-RAS with GIS in Overland Flow Modeling and Flood Hazard Zone Mapping within the Kan River Watershed of Tehran. AGU24. https://agu.confex.com/agu/agu24/prelim.cgi/Paper/1594722
29. Murphy PNC, Ogilvie J, Arp P. Topographic modelling of soil moisture conditions: a comparison and verification of two models. European Journal of Soil Science. 2009; 60(1): 94–109. doi: 10.1111/j.1365-2389.2008.01094.x
30. Estelaji F, Zahedi R, Gitifar A, et al. Integrating HEC-RAS, GIS, and LISREL for assessing and enhancing urban building resilience against flood threats: Comprehensive model and analysis. Heliyon. 2024; 10(20): e39463. doi: 10.1016/j.heliyon.2024.e39463
31. Mishra SK, Singh VP. Soil Conservation Service Curve Number (SCS-CN) Methodology. Springer Netherlands; 2003.
32. Young AF, Papini JA. How can scenarios on flood disaster risk support urban response? A case study in Campinas Metropolitan Area (São Paulo, Brazil). Sustainable Cities and Society. 2020; 61: 102253. doi: 10.1016/j.scs.2020.102253
33. Huang M, Gallichand J, Dong C, et al. Use of soil moisture data and curve number method for estimating runoff in the Loess Plateau of China. Hydrological Processes. 2006; 21(11): 1471–1481. doi: 10.1002/hyp.6312
34. Daly C, Halbleib M, Smith JI, et al. Physiographically sensitive mapping of climatological temperature and precipitation across the conterminous United States. International Journal of Climatology. 2008; 28(15): 2031–2064. doi: 10.1002/joc.1688
35. Hu C, Wright AL, Lian G. Estimating the Spatial Distribution of Soil Properties Using Environmental Variables at a Catchment Scale in the Loess Hilly Area, China. International Journal of Environmental Research and Public Health. 2019; 16(3): 491. doi: 10.3390/ijerph16030491